NATIONAL UNIVERSITY OF SCIENCE AND TECHNOLOGY POLITEHNICA BUCHAREST

Doctoral School of Electronics, Telecommunications and Information Technology

Decision No. 92 **from** 05.10.2023

Ph.D. THESIS
SUMMARY

Ileana Mădălina CIUCĂ

METODE PENTRU
ANALIZA DATELOR POLSAR MONOSTATICE ȘI BISTATICE

METHODS FOR MONOSTATIC AND BISTATIC POLARIMETRIC
SAR IMAGE ANALYSIS

THESIS COMMITTEE

Prof. Dr. Eng. Ion MARGHESCU National University of Science and Technology Politehnica Bucharest	President
Prof. Dr. Eng. Silviu CIOCHINĂ National University of Science and Technology Politehnica Bucharest	PhD Supervisor
Prof. Dr. Eng. Ioan NICOLAESCU Military Technical Academy „Ferdinand I" of Bucharest	Referee
Prof. Dr. Eng. Ion BOGDAN Technical University „Gheorghe Asachi" Iaşi	Referee
Prof. Dr. Eng. Andrei ANGHEL National University of Science and Technology Politehnica Bucharest	Referee

BUCHAREST 2023

Abstract

Polarimetric Synthetic Aperture Radar (PolSAR) data records the scattering diversity by measuring the electromagnetic response in two orthogonal polarization bases. The interaction of the microwaves with both anthropogenic and natural media can modify the incident polarimetric state. PolSAR applications exploit the incident-scattering polarization dependence, which was proven as an important asset, especially for detection and classification.

The main aim of this thesis is to contribute to the analysis of full-polarimetric PolSAR data. In line with expected technological developments in the area of radar instruments, the case of bistatic geometry is discussed. Throughout the work, the matrix formalism has been assumed for data representation and processing. Because PolSAR scattering matrices have properties which depend on the scattering geometry, the methods proposed in the thesis are applicable to the most general case, i.e., with non-reciprocal data (monostatic or bistatic).

The thesis proposes two frameworks for the scattering matrix based on the Real Representation and the Polar Decomposition. The two parts are complementary, with models based on an algebraic vs. geometric processing, on a conjugate similarity vs. similarity factorization or on a coherent vs. incoherent application context. The first contribution is oriented towards the study of the conjugate similarity in PolSAR by the use of the Real Representation. The second contribution is based on the properties of the polar decomposition and the Riemannian geometry of positive semidefinite matrices. Here, a geometric clustering algorithm, combining the k-means and a Riemannian geodesic distance is introduced.

Airborne, monostatic, PolSAR datasets alongside simulated monostatic and bistatic polarimetric data are used for testing the proposed methods.

Table of contents

Acronyms

AIRM Affine Invariant Riemannian Metric

BSA Backscatter Alignment

CEM Computational Electromagnetic

dual-pol Dual Polarimetric

EM Electromagnetic

full-pol Full Polarimetric / Quad Polarimetric

FSA Forward Scattering Alignment

HPD Hermitian Positive Definite

ICA Independent Component Analysis

ICTD Incoherent Target Decomposition

PolSAR Polarimetric Synthetic Aperture Radar

PolInSAR Polarimetric Interferometric Synthetic Aperture Radar

RCS Radar Cross-Section

RR Real Reprezentation

RRSM Real Reprezentation Scattering Matrix

Rx Receiver

SAR Synthetic Aperture Radar

SM Scattering Matrix

SSVD Symmetric Singular Value Decomposition

SVD Singular Value Decomposition

Tg Target

Tx Transmitter

Chapter 1

Introduction

1.1 Presentation of the field of the doctoral thesis

Remote sensing allows the detection and monitoring of an object's physical characteristics, at a distance. Microwave remote sensing is the branch which uses for this study electromagnetic signals belonging to the radar (or, microwave) frequency domain ($\approx$ 300 MHz - 300 GHz). It is further divided into active and passive sub-branches, depending whether the sensor carries, or not, its own signal source.

Active microwave remote sensing is nowadays a conventional technology in Earth observation applications, seen as a complement to the optical technology, e.g., due to its unrestricted imaging ability (day or night, all weather). The most popular radar remote sensing implementation is through the Synthetic Aperture Radar (SAR) technology. By combining several, adjacent, multi-angle observations, SAR has the ability to provide high-resolution (nowadays, even around tens of cm) image-like visualizations of an area's radar backscattering return.

There has been an increased interest in the last decade in improving multi-platform (synthetic aperture) radar systems. The 2010 launch of TerraSAR-X's twin satellite, TanDEM-X, led to the creation of the first single-pass interferometric space-based SAR instrument. These efforts highlighted the technological maturity and potential advantages of multi-platform diversity, such as the ability to perform simultaneous acquisitions from distinct positions in space in one single-pass. In addition, the numerous preparatory and exploratory scientific studies provided through/for the TerraSAR-X/TanDEM-X couple have generated a new surge of interest towards the development of bistatic/multistatic systems.

By combining sets of multiple observations of the same area, the primary form of diversity for all remote sensing applications is multi-temporal. With satellite instruments, the revisit time is periodic and new acquisitions are acquired by multi-pass. Other forms of diversity are possible in microwave remote sensing.

Frequency, polarization and spatial (or, multi-platform) become accessible when the radar sensor is equipped with specialized instrumentation.

The polarization is a wave property defined in a plane transverse to the propagation direction. As a research subject it is studied across disciplines and especially in domains involving electromagnetic radiation. The polarization may carry the signature of an absorption/scattering process, quantified through measurable changes in perpendicular directions of the transverse plane.

In radar polarimetry, the active instrument is the one fixing the polarization at emission, which will usually be modified by the interaction of the radiation with the Earth surface, measured at one or more frequencies. Polarimetric SAR (hereafter, PolSAR) offers access to a multidimensional, simultaneous set of measurements of the radiation reaching the sensor. Crop monitoring, land use/land cover classification, persistent scatterers detection in urban environment, or the study of glaciers and Arctic ice are among its principal applications.

This thesis focuses on the study of polarimetric radar diversity with datasets obtained by acquisition in monostatic or bistatic geometry. New methods and algorithms for PolSAR processing (linear polarization) are proposed. These are developed around two working hypotheses, aiming to address current challenges in radar polarimetry, as follows.

- **Context:** Between the end of the 20th century and the beginning of the 21st century, polarimetric diversity was most often combined with multi-temporal or multi-frequency diversity to obtain composite data sets. Most of the PolSAR methods are based on the algebraic model of reciprocal data, meaning they have been developed and tested mainly using monostatic data.

  Challenge: Due to the growing interest in bistatic/ multistatic radar platforms, it is expected that such PolSAR data will become accessible in the future (both as single acquisitions and in composite sets that will exploit the spatial diversity offered by multi-platform geometries).

  Working hypothesis within the thesis: The polarimetric data should no longer be constrained by the monostatic reciprocity property.

- **Context:** The progressive decrease of the size of resolution cells in radar images has been achieved through technological and data processing developments. This steady improvement of the spatial resolution has made SAR images attractive in various practical applications and competitive with optical sensors.

  Challenge: However, it has been shown that statistical model-based methods used in SAR/PolSAR need to be modified when working with high spatial resolution data and many models have been eventually proposed to accurately represent these statistics [13].

Working hypothesis within the thesis: The difficulty of choosing an optimal model could be solved by proposing techniques that do not rely solely on the statistical distribution of the data.

1.2 Content of the doctoral thesis

Below is a brief summary of the work presented in this thesis.

Chapter 2 sets the main theoretical framework. For this, it introduces the elementary descriptors of wave polarization, compares the radar versus optical scattering alignment conventions and the matrix versus vector PolSAR formalism, which are at the core of most analysis methods for coherent and incoherent decomposition.

Chapter 3 develops from the following question: Which processing is adequate if one operates under the radar convention, i.e., Backscattering Alignment (BSA), adopts a matrix formalism computation and deals with radar observations which are not reciprocal (inherent property, not the result of measurement errors)?

A purely mathematical perspective is necessary at first. We introduce the conjugate similarity transformation (hereafter, consimilarity) and propose a solution based on the real representation. The results returned by this method are proven to match the ones from the non-negative factorization of the squared scattering matrix, only in the case when the matrix is reciprocal. The method reveals complex-valued solutions for the case of some non-reciprocal scattering matrices. The chapter then explores practical applications for the real representation, particularly through its eigen-decomposition. Monostatic and bistatic wide-angle polarimetric simulations of two coherent targets are obtained and investigated on the premise of pursuing a concrete link between scattering geometry, nonreciprocity and the complex (con)eigenvalues.

Chapter 4 continues to explore applications under the PolSAR matrix formalism, but considers now an operation based on similarity, i.e., the polar decomposition. A geometric perspective is adopted in this chapter. The polar decomposition factors are seen not only as algebraic products, but using well-known results in information geometry, as matrix terms embedded into a manifold. Eventually, the proposed method uses exclusively the Hermitian positive definite factor and operations onto its associated Riemannian manifold. When assuming the PolSAR vector formalism, the classical incoherent target decompositions (ICTDs) operate with the sample covariance matrix, which is generally estimated as a weighted

sum of vector inner products. Differently, we propose to use the intrinsic geometric mean of Hermitian positive definite matrices, followed by a partitional clustering algorithm having a geodesic distance for intra/inter-cluster attribution.

Two particularly appealing properties are that the algorithm does not require any assumption of the data statistical models and does not modify, at any step, the algebraic matrix structure. Qualitative and quantitative tests are performed using real and simulated monostatic datasets. Despite this choice, the technique could be applied to the most general type of polarimetric diversity, i.e., bistatic full-polarimetric.

Chapter 5 provides an overall focus on the thesis' contributions and proposes an outlook on future work. Contributions into peer-reviewed publications and conferences during the time-frame of this thesis are also listed.

To improve readability, retain the focus of the main chapters on personal contributions, but still provide extensive clarifications where needed, proofs and other extra material are transferred at the end of the thesis into **Annexes A-H**.
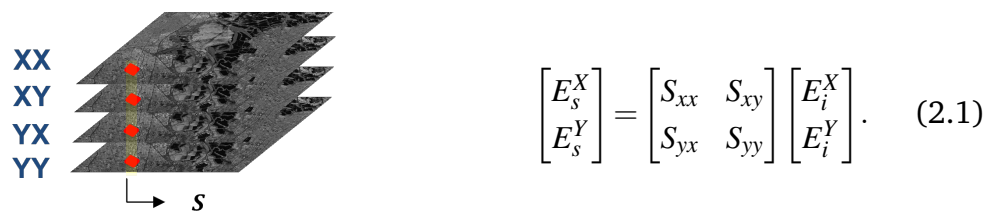
Chapter 2

Polarimetric Radar Diversity

The polarization of a wave is generally defined by the oscillation direction of the electric field components in the transverse plane. It is often understood as the figure "that the extremity of a (specified) vector field draws as a function of time". Otherwise, the polarization of an antenna is "that of the plane wave it radiates at large distances in a given direction" [1, 2].

Conventional radar imaging assumes a *monostatic* geometry, in which the transmitter and receiver units are co-located. In a *bistatic* system, the transmitter and receiver are located in different places and have a considerable (several orders of magnitude greater than the wavelength) separation (baseline) between them. If the transmitter and receiver are just separate pieces of equipment, but placed close together, the geometry is called *quasi-monostatic*.

A target illuminated in the scene by the radar instrument is known to behave as a polarization state modifier [16].

For a generic set of polarization bases (X-Y), the change between the incident and backscattered field components is described through the scattering matrix (2.1), $\mathbf{S} \in \mathbb{C}^{2\times 2}$:

$$\begin{bmatrix} E_s^X \\ E_s^Y \end{bmatrix} = \begin{bmatrix} S_{xx} & S_{xy} \\ S_{yx} & S_{yy} \end{bmatrix} \begin{bmatrix} E_i^X \\ E_i^Y \end{bmatrix}. \quad (2.1)$$

Fig. 2.1 **Full-polarimetric radar observations.**

Targets are expected to have a deterministic or non-deterministic scattering response. A deterministic target (or single scatterer) has a stable polarization response over time, which is entirely characterized by its scattering matrix. In contrast, the scattering response of a non-deterministic target does not remain stable and is modeled using stochastic processes. This scatterer is also known as partial or distributed, with dimensions expected to span several resolution cells [34, 41].

2.1 Radar and optical coordinate systems

In radar polarimetry, the polarization is a property of both the incoming electromagnetic signal and of the active device which emits the radar signal and performs the measurements. As suggested by the IEEE Antenna Standards, the polarization of an antenna is that of the wave it radiates, which implies that in the receiving case, the "coordinate systems used to describe the polarization of the antenna and the incoming wave are oriented in opposite directions" [2]. As so, there is a radar-specific, *antenna-oriented* convention known as the Backscatter Alignment (BSA) [28].

By contrast, in optics and other domains where polarimetry is used, the conventional coordinate system is the Forward Scattering Alignment (FSA). Comparing BSA and FSA, the unit vector on the receiving path of the former is represented with a 180° inversion of orientation, with respect to the latter [28].

The distinction between the two is marked in mathematical terms by a conjugation operation, introduced on one side of the equality transformation equation. In this context, the base change relations of the two conventions are different: whereas FSA exploits similarity transformations performed on the Jones matrix, BSA exploits conjugate similarity transformations performed on the Sinclair (i.e., radar scattering) matrix [21, 32, 41].

2.2 Similarity and conjugate similarity transformations

Similarity and conjugate similarity are two equivalence relations for complex matrices. Considering three matrices $\mathbf{A}, \mathbf{B}, \mathbf{C} \in \mathbb{C}^{n \times n}$, one can write:

Tabel 2.1 General equations of similarity and consimilarity.

similarity	con(jugate) similarity
$\mathbf{A}\mathbf{V} = \mathbf{V}\mathbf{B}$	$\mathbf{A}\mathbf{X} = \mathbf{X}^{*}\mathbf{C}$

Matrices $\mathbf{V}$ and $\mathbf{X} \in \mathbb{C}^{n \times n}$ are referred as the similarity and consimilarity transformation matrices. However, using a real matrix $\mathbf{X} \in \mathbb{R}^{n \times n}$ (e.g., an orthogonal rotation matrix), the consimilarity operation changes into a similarity one.

If matrices $\mathbf{V}$ and $\mathbf{X}$ are unitary ($\mathbf{V}^{\mathsf{H}}\mathbf{V} = \mathbf{V}\mathbf{V}^{\mathsf{H}} = \mathbf{I}$ and $\mathbf{X}^{\mathsf{H}}\mathbf{X} = \mathbf{X}\mathbf{X}^{\mathsf{H}} = \mathbf{I}$) the two operations are assimilated as an eigen-decomposition and respectively, as a coneigen-decomposition (Table 2.2).

For a symmetric complex matrix $\mathbf{A}$, $\mathbf{X}$ is always unitary and the conjugate similarity is always equivalent to the unitary congruence [20]:

Tabel 2.2 Eigenvalues/Eigenvectors and conjugate counterparts.

eigenvalue/eigenvector	coneigenvalue/coneigenvector
$\mathbf{A}\mathbf{v_n} = \lambda_n \mathbf{v_n}$	$\mathbf{A}\mathbf{x_n} = \xi_n \mathbf{x_n^*}$

$$\begin{aligned}
\mathbf{\Gamma} &= (\mathbf{X^*})^{-1}\mathbf{AX} = (\mathbf{X^{-1}})^*\mathbf{AX} \\
&= (\mathbf{X^H})^*\mathbf{AX} = \mathbf{X^T}\mathbf{AX}.
\end{aligned}$$

(2.2)

Both the requirement of the conjugate similarity transformation and the ability to claim the symmetry of the monostatic scattering matrix $\mathbf{S}$ are by-products of imposing the BSA convention. The second weakens the first, so that monostatic scattering matrices verifying reciprocity are diagonalized under unitary congruence [19, 33, 23]. While this is distinct from the well-known unitary similarity diagonalization, the computation is always possible and the mathematical formalism is available in PolSAR from the early works of Graves [17], better known in the mathematical literature as the Autonne-Takagi factorization [18]. This thesis looks at the case where matrices are no longer symmetric and, as a result, the Graves factorization can no longer be applied.

With symmetric scattering matrices, $\mathbf{S} = \mathbf{S^T}$, the eigenvalues of the Graves matrix, $\mathbf{G} = \mathbf{S^H}\mathbf{S} = \mathbf{S^{T*}}\mathbf{S} = \mathbf{S^*}\mathbf{S}$, are equal to the squared coneigenvalues, whilst its eigenvectors are equal to the coneigenvectors in this same case [31]. Moreover, if the eigenvalues of $\mathbf{G}$ are equal, this method can no longer be used to solve Takagi's factorization [30, 18].

The unitary congruence of symmetric scattering matrices can also be assimilated to the Symmetric form of the Singular Value Decomposition (the SSVD). For the bistatic case, the SVD is directly proposed as the recommended decomposition throughout the literature.

It extracts from the scattering matrix two unitary transformations, one characterizing the transmitter-target path (Tx-Tg) and the other the target-receiver path (Tg-Rx) [11]. When considering the consimilarity operation, these two transformation matrices can only be conjugate pairs. That is why, the consimilarity is sometimes referred as a special case of the SVD. The connections between the above-mentioned transformations are shown in Figure 2.2.

The general conjugate similarity transformation for non-reciprocal scattering matrices has not yet been sufficiently studied in the field of radar polarimetry. In the first part of the thesis, we argue it can provide new information for the analysis of scattering matrices.
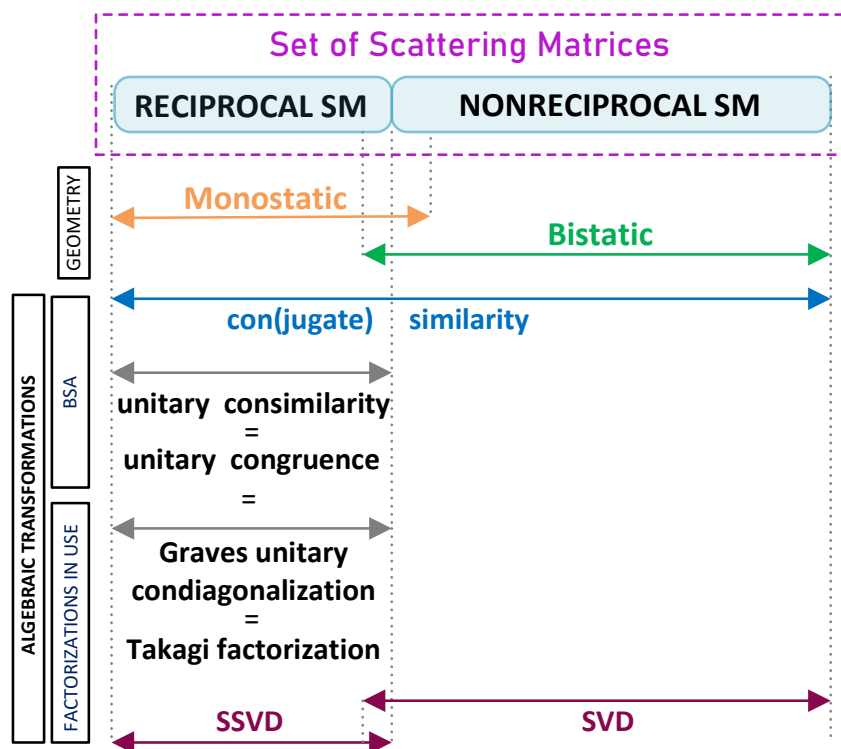
Fig. 2.2 Conjugate similarity and SVD operations for reciprocal and nonreciprocal scattering matrices.

2.3 Coherent and incoherent polarimetric decompositions

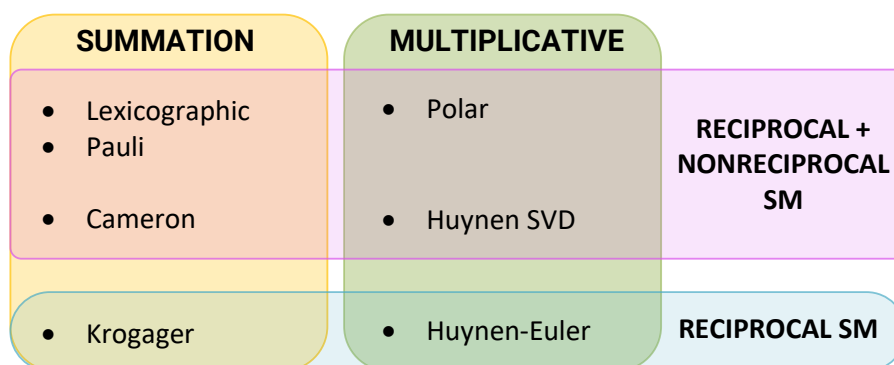Fig. 2.3 **Classification of coherent decompositions**.
Horizontal axis: factorization type (summation and multiplicative).
Vertical axis: applicability to reciprocal and nonreciprocal scattering matrices.
Acronyms: SVD: Singular Value Decomposition.

The information potentially contained in multi-polarization observations is exploited using decomposition techniques, which form a core theory in PolSAR.

These techniques are used to separate the polarimetric signature captured by the radar instruments into a combination of simpler scattering responses, to which a physical significance can be associated. They can be partitioned into coherent and incoherent methods (Figure 2.3).

- **Coherent decomposition**
  The coherent methods are divided into two main classes, as they can decompose the scattering matrix via a summation or a multiplicative factorization [28].

  A decomposition by addition uses a set of elementary matrices that form the decomposition basis. The Pauli matrices are, for example, the standard basis for the case of 2×2 matrices. These matrices have a physical interpretation in PolSAR: odd echo, even echo, diffuse and asymmetric mechanisms. Only the first three components are non-zero when a reciprocal scattering matrix is decomposed.

  A multiplicative decomposition (such as the diagonalization) uses algebraic operations to extract elementary factors. The Huynen [22] and the polar decomposition [39] are proposed as examples. The main developments proposed in this thesis are related to the branch of coherent decomposition. More specifically, the contributions are based on appropriate multiplicative factorization methods for reciprocal and non-reciprocal scattering matrices.

- **Incoherent decomposition**
  The target scattering vector provides an equivalent representation of the polarimetric information [10, 11]. Its connection with the diffusion matrix can be represented by a projection into the set of N elements of a summation basis $\{\Psi\}$ (Pauli, $(\cdot)_{\mathscr{P}}$, or lexicographic, $(\cdot)_{\mathscr{L}}$, are generally used):

  $$\mathbf{k} = \mathrm{Vect}(\mathbf{S}) = \frac{1}{2}\mathrm{Tr}(\mathbf{S}\Psi) \qquad (2.3)$$

  I. *Full-polarimetric data*
     Bistatic observations generally use a complete set of four basis matrices, whereas in the monostatic case (under the reciprocity assumption), the set of (2×2) basis matrices is reduced to only three.

  II. *Dual-polarimetric data*
     For dual-polarimetric data, whether the geometry is monostatic or bistatic, the target scattering vector has the same dimension, only 2×1 (which corresponds to an incomplete set of two basis matrices). In the case of linear polarization, there are three possible dual-polarimetric combinations: HH-VV, HH-VH and VV-HV.

2.4   Application: Dual-polarimetric bistatic and mono-static VV-HV H-alpha classification

The scattering response of partial/distributed targets is no longer relevant under pixel-level analysis. In the case of older imaging instruments, the larger the area on the ground of a resolution cell, the larger the number of real objects interacting with the radar signal inside this cell.

PolSAR data presents, in this cases, a stochastic nature and the relevant analysis tools require the computation of higher-order moments. The elementary statistical model used for the target scattering vector is that of a circular Gaussian distribution with zero mean [38]. The probability density function associated to the target vector is:

$$p(\mathbf{k}) = \frac{1}{\pi^m \det(\mathbf{C})} \exp\left(-\mathbf{k}^{\mathsf{H}} \mathbf{C}^{-1} \mathbf{k}\right), \tag{2.4}$$

$m \in \{3,4\}$ is the vector dimension, $\mathbf{C} = \mathbb{E}\left\{\mathbf{k}_{\mathscr{L}} \mathbf{k}_{\mathscr{L}}^{\mathsf{H}}\right\}$ represents the (lexicographic) covariance and $\mathbb{E}\{\cdot\}$ is the expectation operator.

It is generally considered that the Gaussian model for the target vector best describes PolSAR data from: a) homogeneous regions or b) for which a large number of elementary targets are present within the resolution cell (under the application of the Central Limit Theorem). This is often the case for medium and low-resolution observations. Because the work presented in the thesis does not make direct references to statistical models, the simple Gaussian case is implicitly assumed (that is, the non-Gaussian case for very high resolution data is ignored). The complex covariance, generally estimated by the spatial mean according to the maximum likelihood criterion, $\hat{\mathbf{C}}$, then follows a complex Wishart distribution with a probability density function:

$$p(\hat{\mathbf{C}}) = \frac{L^{qL} (\det\hat{\mathbf{C}})^{L-q}}{(\det\mathbf{\Sigma})^L \Gamma_q(L)} \exp\left(-L \cdot \mathrm{Tr}(\mathbf{\Sigma}^{-1}\hat{\mathbf{C}})\right), \tag{2.5}$$

where $\Gamma_q(L) = \pi^{\frac{q(q-1)}{2}} \prod_{i=0}^{q-1} \Gamma(L-i)$, $\Gamma(\cdot)$ represents the standard Euler gamma function, q is the covariance matrix order and $\mathbf{\Sigma} = \mathbb{E}\{\hat{\mathbf{C}}\}$.

The Entropy-alpha classification is, probably, the most popular PolSAR incoherent decomposition. The entropy (H) is a eigenvalues-based parameter used to describe the randomness of a scattering target, while alpha (α) is the average value of orientation angles (α_i) obtained from the eigenvectors. These parameters are written down as follows:

$$H = -\sum_{i=1}^{m} P_i \log_m P_i \quad 0 \le H \le 1 \quad (2.6) \qquad \alpha = \sum_{i=1}^{m} P_i \alpha_i \quad 0° \le \alpha \le 90° \quad [deg.] \quad (2.7)$$

$$P_i = \frac{\lambda_i}{\sum_{j=1}^{m} \lambda_j} \quad 0 \le P_i \le 1; \quad 1 \le i \le m \quad (2.8)$$

If the same definitions and formulas for H and α apply regardless of the polarimetric dimension of the data (full or dual) [11], their interpretation of scattering properties changes, in particular for alpha, which loses its rotation invariance property in dual-pol [12, 3]. This is a known result, mentioned in the literature, for the monostatic case.

The choice of multi-polarimetric diversity is often subject to trade-offs in real systems, so dual polarimetry may be often preferred. The application section of this chapter presents a dual polarization $H - \alpha$ comparison using simultaneously recorded monostatic and bistatic polarimetric data. The experimental results indicate that the dual-pol scattering mechanisms involved in the monostatic and bistatic geometries are sufficiently different that an increase in the alpha value is observed in the bistatic case for most of the scatterers in the image (Fig. 2.4).

Then, the remainder of the thesis focuses entirely on using a complete polarimetric framework.
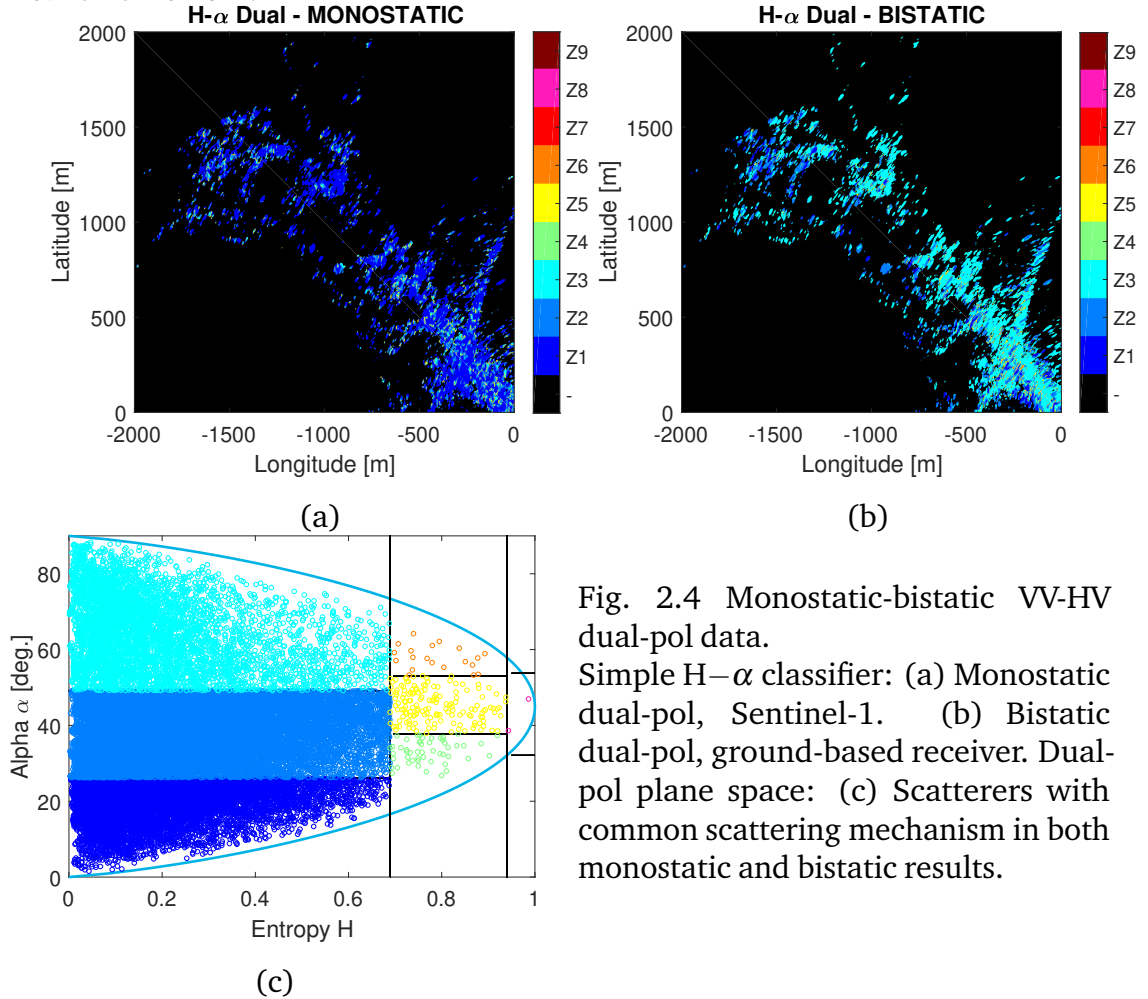

(a)

(b)

(c)

Fig. 2.4 Monostatic-bistatic VV-HV dual-pol data.
Simple $H - \alpha$ classifier: (a) Monostatic dual-pol, Sentinel-1. (b) Bistatic dual-pol, ground-based receiver. Dual-pol plane space: (c) Scatterers with common scattering mechanism in both monostatic and bistatic results.

Chapter 3

Real Representation Scattering Matrix

Transforming a general scattering matrix through a con(jugate) similarity operation is a necessary mathematically procedure under the radar Backscatter Alignment. Generally, the interest is in recovering the factorization terms, which under diagonalization are known as con(jugate) eigenvalues and con(jugate) eigenvectors. These are the two pairs $(\xi_k, \mathbf{x_k})$, $k = \{1,2\}$ which verify:

$$\mathbf{S}\mathbf{x_k} = \xi_k \mathbf{x_k^*} \tag{3.1}$$

As discussed in the previous chapter, for non-reciprocal matrices, this operation can no longer be reduced to unitary congruence. One of the aims of this chapter is to discuss the challenges and benefits of using the consimilarity transformation in this case. Known PolSAR techniques apply either the Graves/Takagi unitary congruence operation for reciprocal matrices or the SVD for non-reciprocal matrices, with a clear distinction that the former applies to monostatic and the latter to bistatic data. The work presented in this section offers a necessary complement, for example when non-reciprocal monostatic data is available or as an alternative to the SVD method for the bistatic case.

3.1 Real Representation Scattering Matrix

To the best of our knowledge, the methods available in the literature for solving a conjugate similarity transformation between two complex matrices are not direct. They are based on mappings to an equivalent space where the conjugate similarity can be evaluated as a similarity equation. Possible mappings present in the literature are based either on the complex product between the scattering matrix and its complex conjugate [20], or using a certain type of block matrices [8, 24].

We prefer to write the scattering matrix using its Real Representation (RR) [25, 9]. This matrix, $\mathbf{S_{RR}} \in \mathbb{R}^{4 \times 4}$ - addressed hereafter as the Real Representation Scattering Matrix (RRSM), is composed of blocks containing the real and imaginary parts, operators $Re(\cdot)$ and $Im(\cdot)$, respectively, of the original complex matrix $\mathbf{S}$.
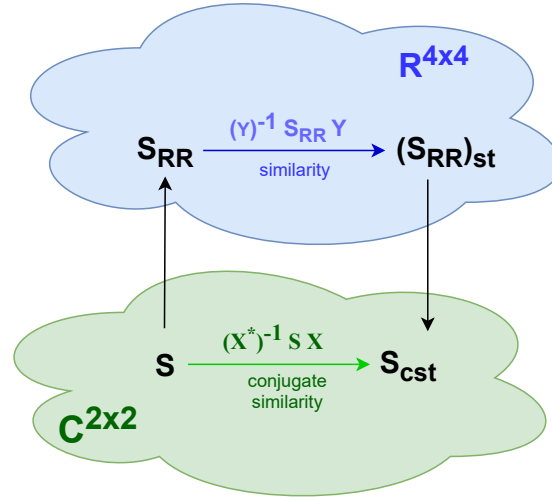

Fig. 3.1 Mapping the consimilarity operation between two complex matrices ($\mathbf{S}$, $\mathbf{S_{cst}}$) to that of ordinary similarity between two real matrices ($\mathbf{S_{RR}}$, $\mathbf{S_{RR_{st}}}$).

$$\mathbf{S_{RR}} = Re(\mathbf{S}) + j Im(\mathbf{S}) = \begin{bmatrix} Re(\mathbf{S}) & Im(\mathbf{S}) \\ Im(\mathbf{S}) & -Re(\mathbf{S}) \end{bmatrix}. \tag{3.2}$$

3.2 Real concanonical form and properties of the real representation

The eigenvalues of the RRSM and the coneigenvalues of the scattering matrix share similar properties: a) they are found in positive-negative pairs which b) are of the same algebraic type (Table 3.1).

When at least two eigenvalues of $\mathbf{S_{RR}}$ are equal, it may not be possible to have a diagonal form for $\mathbf{S_{RR_{st}}}$. The canonical Jordan form may be used in this case [20] (for notations, please check Appendix C of the thesis):

$$(\mathbf{S_{RR}})_{\mathbf{J}} = (\mathbf{S_{RR}})_{\mathbf{st}} = \left[\bigoplus_{k_1} \mathbf{J}_{p_{\mathscr{R}}}(\lambda_{k_1}) \right] \oplus \left[\bigoplus_{k_2} \mathbf{J}_{r_{p_{\mathscr{I}}}}(\lambda_{k_2}, \lambda_{k_2}^*) \right]. \tag{3.3}$$

Each positive-negative pair of eigenvalues (with real or complex elements) of the canonical form $(\mathbf{S_{RR}})_{\mathbf{J}}$ will correspond to a coneigenvalue (the positive

Tabel 3.1 Eigenvalues of RRSM and con-eigenvalues/eigenvectors of the SM.

| | RRSM | SM | |
	eigenvalues	coneigenvalues	coneigenvectors
real	**distinct** pairs $\{\lambda_1,\lambda_2,-\lambda_1,-\lambda_2\}$	distinct real $\{\xi_1,\xi_2\}$	independent, orthogonal
	equal pairs $\{\lambda,\lambda,-\lambda,-\lambda\}$	equal real $\{\xi,\xi\}$	a. independent, orthogonal or b. independent, with one coneigenvector and one generalized coneigenvector
complex	**conjugate** pairs $\{\lambda,\lambda^*,-\lambda,-\lambda^*\}$	complex $\{\xi,\xi^*\}$	one coneigenvector and one generalized coneigenvector

value of the pair is chosen). For example, for a real pair of eigenvalues $(\lambda,-\lambda)$, corresponds a positive real coneigenvalue $\xi = \lambda$, $\lambda > 0$. A positive-negative complex pair is associated with a complex coneigenvalue. The existence of complex eigenvalues provides a complete characterization of the case of inhomogeneous Sinclair matrices (with respect to the consimilarity). For reciprocal scattering matrices, the Graves-Takagi factorisation is the standard operation for obtaining the coneigenvalues (Figure 2.2).
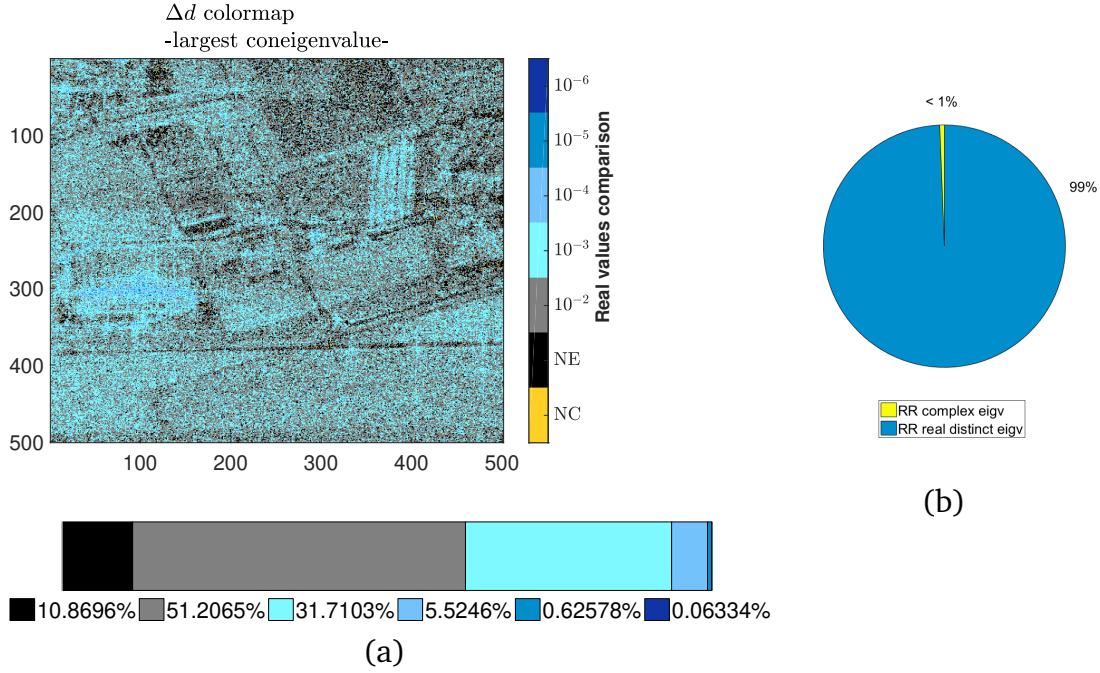
Fig. 3.2 Comparison of absolute difference (Δd) between values obtained by the Graves method and values obtained using the RR method - Largest coneigenvalue (ξ_1). (a) Color-coded representation. (b) Percentage of RRSM eigenvalues: real vs. complex.
Legend acronyms: NC (yellow) = Not Compared, NE (black) = Not Equal. Pixels are assigned in the following gray and blue classes if the values obtained by the two methods are equal under a tolerance δ_d ranging from 10^{-2} to 10^{-6}.

For the monostatic case, the number of matrices returning complex coneigenvalues is generally expected to be small. The polarimetric Brétigny dataset (monostatic, X-band), considered as example, verifies this hypothesis (Figure 3.2b). Figure 3.2a) shows the numerical comparison between the coneigenvalues estimated by the two numerical methods (Graves-Takagi and RR) for the reciprocal case (with real values only). In a large percentage, the values obtained are equivalent under a tolerance $\delta_d \leq 10^{-2}$.

The chapter then goes on to analyze the connection between the non-reciprocity factor of the scattering matrix [26], $\zeta = \frac{1}{\sqrt{2}}\frac{(S_{vh}-S_{hv})}{\|\mathbf{S}\|_F}$, and the complex coneigenvalues. Notation $\|\mathbf{S}\|_F = \left(\sum_{i,j\in\{h,v\}}|S_{ij}|^2\right)^{1/2}$ corresponds to the Frobenius norm. In this part of the chapter, the methodology uses simulated (monostatic and bistatic, C-band) polarimetric scattering responses from two metallic objects, considered as distinct targets in the resolution cell: a dihedral and a square plate. The scattering response of these two targets correspond in the polarimetric theory to two elementary scattering mechanisms: double and single bounce, respectively.

An electromagnetic computation software is used to obtain the scattered electric field responses from which scattering matrices are estimated, for each object, over a wide range of angular values.

In this short summary, only the dihedral example is considered. The simulated monostatic data is verified by two different methods: comparison of the simulated radar cross-section with analytic results (Figure 3.3) and the verification of estimated **S** matrices using polarimetric parameters (Table 3.2). The same resources are not currently available for the bistatic case, so the results of the bistatic simulation are not checked beforehand. Finally, the estimated (monostatic and bistatic) scattering matrices are put into the form of the real representation and the percentages of the different RRSM eigenvalues types are computed.

■ **Dihedral(monostatic case)**

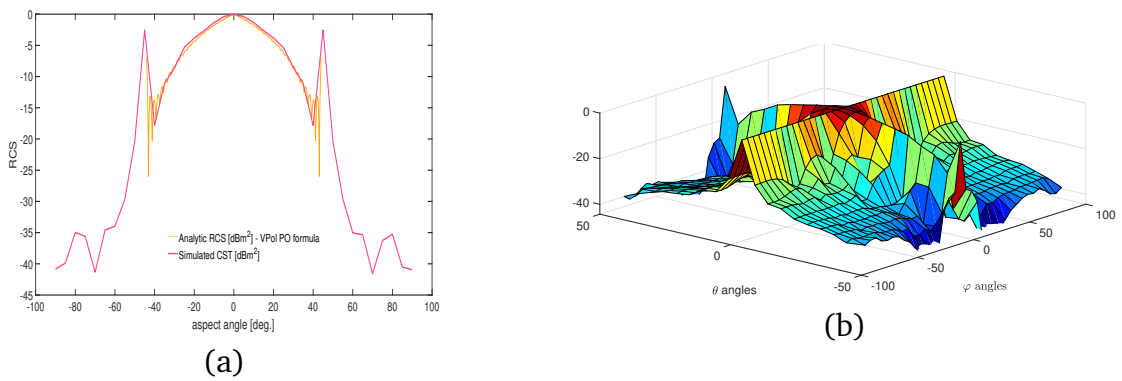I. *Radar cross section verification*

(a)

(b)

Fig. 3.3 **Dihedral - Monostatic result** (Vertical Polarisation). (a) RCS Comparison: Values simulated by CEM software and by analytic formulas (1D, [dBm^2]). (b) Normalized absolute values of CEM simulated electric field E_s (3D, [dB(V/m)]).

II. *Verification by polarimetric parameters of the scattering matrices estimated by simulation*

Tabel 3.2 **Monostatic dihedral**. Evaluation based on angular polarimetric descriptors. Percentage distribution of estimated values in $10°$ intervals between $[0°, 90°]$ (for all observation directions in the investigated range).

	90 − 80	80 - 70	70 - 60	60 - 50	50 - 40	40 - 30	30 - 20	20 - 10	10 - 0
α_{Cloude} [11]	28.7 %	18.2 %	12.8 %	9.8 %	15.1 %	8.53 %	4.03 %	1.42 %	1.42 %
α_{TSVM} [40]	28.7 %	17.5 %	11.8 %	9.8 %	12.95 %	11.7 %	4.7 %	1.42 %	1.42 %

For approximately 45% of the scattering directions, the values of the polarimetric descriptors (α_{Cloude} and α_{TSVM}) vary with less than $20°$ degrees around the theoretical value (i.e., $90°$) associated to the dihedral's scattering mechanism. Although this shows that the dihedral is generally a stable scatterer, there are also observation directions for which the obtained values indicate different scattering mechanisms. For both polarimetric parameters, the results are comparable.
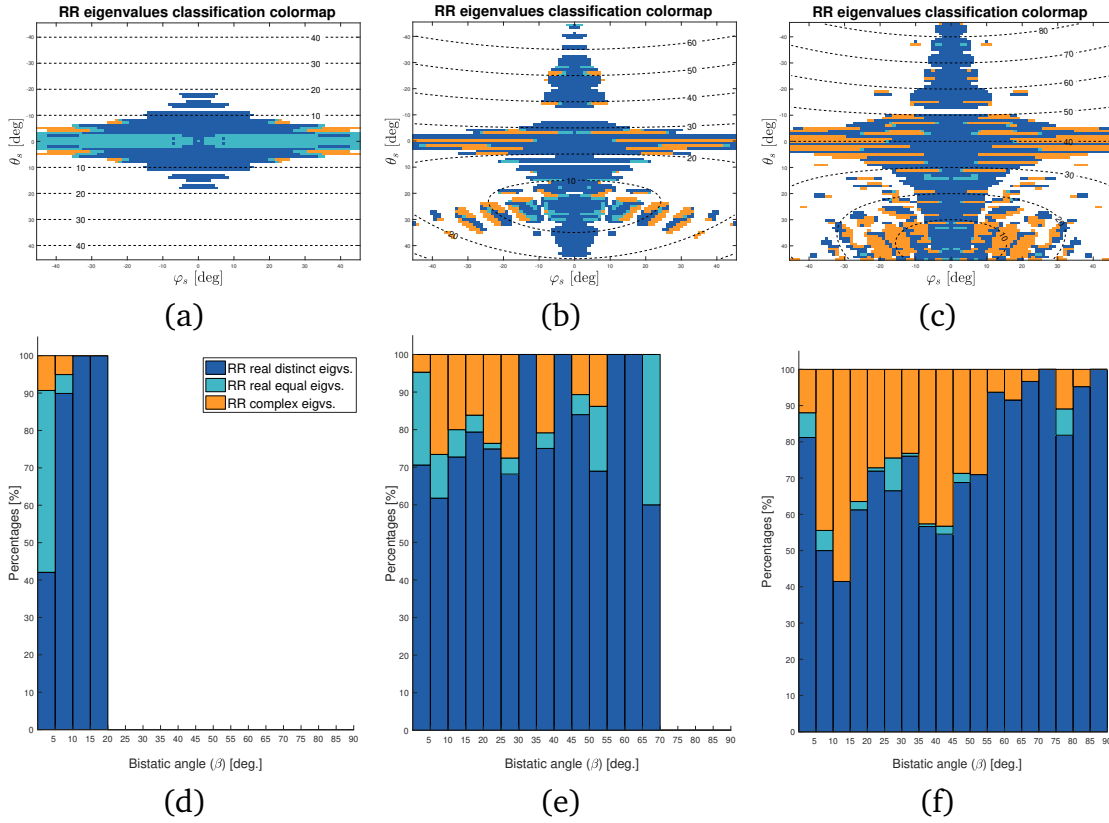
Fig. 3.4 **Dihedral - Bistatic result**
Incidence directions : col. 1 : $\{\theta_i = 0°, \varphi_i = 0°\}$, col. 2 : $\{\theta_i = 25°, \varphi_i = 0°\}$, col. 3 : $\{\theta_i = 40°, \varphi_i = 0°\}$. (a)-(c) RRSM eigen-classification. (d)-(f) RRSM eigen-classification in relation to the bistatic angle, $\beta \in [0°, 90°]$.

■ **Dihedral (bistatic case)**

The results obtained from the bistatic simulations, for three incidence directions (and the same range of backscattering directions, $\{\varphi_s \in [-45, 45], \theta_s \in [-45, 45]\}$, as observed in the monostatic case), are illustrated in Figure 3.4.

The dihedral appears to be a more stable target (compared with the plate's bistatic results), but exhibiting complex eigenvalues of the RRSM for certain scattering directions, oblique with respect to the object's bisector.

However, these observations are not sufficient to define a criteria linking the occurrence of such values to the bistatic angle.

It should be pointed out that the RRSM evaluation is incomplete in certain respects. The decomposition of the real representation block matrix is only applied coherently, without statistical averaging. This type of evaluation is therefore not suitable for characterizing distributed targets. Moreover, the influence of coneigen-vectors has been studied to only a limited extent and should be explored further in future work.

Chapter 4

Geometric clustering using the Hermitian polar factor of PolSAR data

This chapter proposes a geometric unsupervised classification algorithm starting from the polar decomposition of the scattering matrix. The method incorporates the computation of the centroid of Hermitian polar factors in the Riemannian manifold.

The simplified diagram of a general PolSAR clustering algorithm is shown in Figure 4.1.
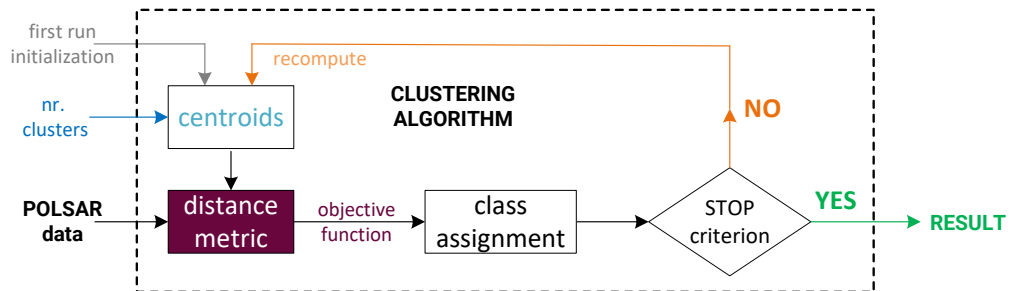

Fig. 4.1 Generic scheme of a centroid-based clustering algorithm for PolSAR data.

4.1 The polar decomposition

The polar decomposition is the factorization of a complex matrix $\mathbf{A}$ into the product of two terms: one unitary and one complex positive (semi-)definite factor. There are two form of the decomposition, depending on the placement of the two factors: (4.1) is the right polar decomposition, while (4.2) is the left polar form.

$$\mathbf{A} = \mathbf{U}\mathbf{H} \qquad (4.1) \qquad\qquad \mathbf{A} = \mathbf{K}\mathbf{U}, \qquad (4.2)$$

where $\mathbf{U} \in \mathbb{C}^{n \times n}$ verifying $\mathbf{U}\mathbf{U}^{\mathsf{H}} = \mathbf{U}^{\mathsf{H}}\mathbf{U} = \mathbf{I}$ is the nearest unitary matrix to $\mathbf{A}$ (in any unitarily invariant norm[1], as argued in [35, 27]). The right/left Hermitian

---

[1]i.e., a norm satisfying $\|\mathbf{A}\| = \|\mathbf{U}\mathbf{A}\mathbf{V}^{\mathsf{H}}\|$

matrices **H** and **K** are equal only if **A** is normal. Regardless of choosing (4.1) or (4.2), the Hermitian term has a unique solution, while the uniqueness of **U** imposes that matrix **A** is nonsingular. Experimental results did not show any difference in preferring one form or the other. The right polar decomposition of the polarimetric scattering matrix **S** is considered by convention in all the results that follow.

- *Complex positive definite factor:*

  The complex positive definite factor **H** verifies $\mathbf{u}^H\mathbf{Hu} \geq 0 \; \forall \; \mathbf{u} \in \mathbb{C}^{2\times 1}$ and presents non-negative, real eigenvalues. One such matrix is equally Hermitian, $\mathbf{H}^H = \mathbf{H}$. In the case where the scattering matrix is complex symmetric (i.e. such as assumed in monostatic), the eigenvalues of the Hermitian factor share a multi-faceted interpretation: coneigenvalues, equal to the singular values, equal to the factors of the Takagi decomposition.

  The study of the properties of each of the decomposition factors led to the conclusion that the Hermitian one can constitute a rotation-invariant input.

  From a geometric point of view, the space of Hermitian Positive-Definite (HPD) matrices takes the form of an open conic manifold. Because this takes the shape of a curbed geometric space, the simple use of Euclidean metrics is no longer optimal for conventional operations (distance measurement, mean value, higher order statistics) on the manifold.

- *Unitary factor:*

  The unitary matrices are the complex counterparts of orthogonal matrices. Many distance functions are unitary-invariant which means that, as their real analogues - the orthogonal matrices, they are known to preserve lengths/amplitudes. The 2×2 group of unitary matrices is known as U(2) and forms a Lie group under matrix multiplication. The latter is an algebraic group having the structure of a smooth manifold.

4.2 On manifolds and Riemannian geometry

A *manifold* $\mathbb{M}$ is a topological space, similar to an Euclidean space at each small vicinity. At any point X on the manifold, the *tangent space $T_X\mathbb{M}$* can be defined (Fig. 4.2).

A metric on the manifold is a choice of inner product at each $X \in \mathbb{M}$. When such an inner product varies smoothly from point to point, it is called a Riemannian metric. The geodesic of a Riemannian space is imposed by this metric, which follows the curvature of the space and thus represents the intrinsic way of measuring distances on the manifold. Other extrinsic metrics can be imposed, but they will not be optimal (see Figure 4.2a).
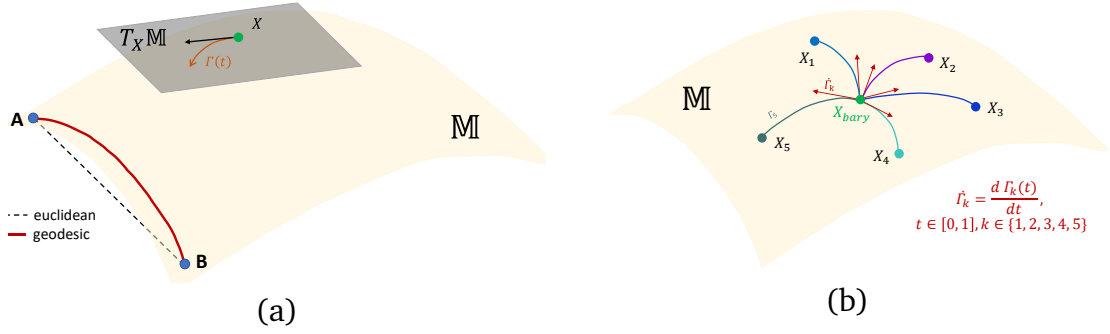
Fig. 4.2 Manifold, tangent space, geodesic (a) Example of a manifold ($\mathbb{M}$) and the tangent space at point X ($T_X\mathbb{M}$). (b) Geodesic and tangent vectors through the set of points $\{X_i\}$, $1 \leq i \leq 5$ and the corresponding barycenter.

The space of Hermitian matrices forms a Riemannian manifold and when endorsed with the Affine Invariant Riemannian Metric (AIRM), the minimum distance between two matrices $\mathbf{A}$ and $\mathbf{B}$ is:

$$d_{\mathbb{P}(n)}(\mathbf{A},\mathbf{B}) = \|\text{Log}(\mathbf{A}^{-1/2}\mathbf{B}\mathbf{A}^{-1/2})\|_F \qquad (4.3)$$

with the geodesic between the points associated to the two matrices, as:

$$\Gamma(t) = \mathbf{A}^{1/2}\left(\mathbf{A}^{-1/2}\mathbf{B}\mathbf{A}^{-1/2}\right)^t\mathbf{A}^{1/2}, \quad t \in [0,1], \quad \Gamma(0) = \mathbf{A} \quad \text{and} \quad \Gamma(1) = \mathbf{B}.$$

The Riemannian barycentre is the minimizer of squared geodesic distances between the set of manifold points associated to a set of HPD matrices (Figure 4.2b). There is no analytic solution to the minimization when more than three matrices are involved, but it has been shown that a minimum exists and is unique when the estimation is carried out throughout optimization methods [6]. Karcher's method, based on a gradient descent implementation, is used in this thesis to obtain the estimate of the Hermitian barycenter [15].

4.3 Geometric clustering with Hermitian factors

It has been more than a decade since the concepts related to the Riemannian manifold of Hermitian matrices began to be applied in PolSAR, but exclusively considering the Hermitian covariance/coherency matrices. Contributions to applications in unsupervised classification and segmentation [14, 44], change detection [5, 4], supervised classification [43, 42] as well as speckle filtering [37, 36] can be mentioned.

The geometric clustering algorithm proposed in this chapter is based on k-means and it exploits two elementary operations: a) the coherent polar decomposition of
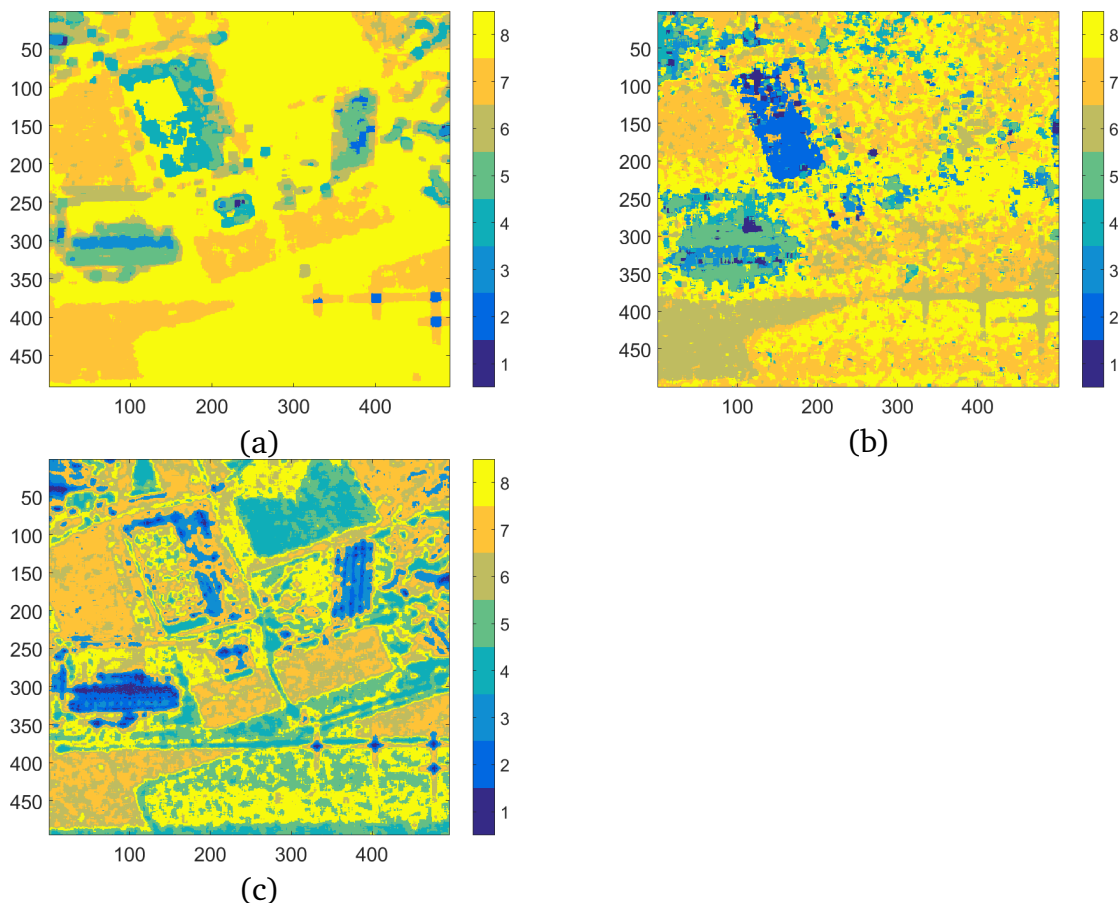
Fig. 4.3 **PolSAR Brétigny data**. (a) Wishart. (b) Angular geodesic k-means. (c) Geodesic Riemannian distance k-means.

PolSAR data and b) an incoherent averaging of **H** factors based on the Riemannian geometry. This framework no longer relies on the use of covariance/coherency matrices, but it exploits more directly the space of scattering matrices. No vectorization of the data is performed (compared with the case when scattering vectors are constructed) and the algorithm is designed to exploit the geometric property of Hermitian factors, which are intrinsically located on the Riemannian manifold. Rather than using a statistical average of the scattering vectors (as in the estimation of the covariance/coherency matrix), a local average (the barycenter) is computed using the manifolds' geodesic metric. The algorithm does not modify the (algebraic/geometric) structure of the input scattering matrices.

Monostatic polarimetric data (real data for qualitative tests and simulated data for quantitative tests) is used to evaluate the proposed method. Tests on real PolSAR data show that the final classification better preserves the texture information from the original images. For example, an improvement is observed in the separation of areas having much lower intensities (as for example, on certain vegetation fields in the Brétigny data, Figure 4.3).

Chapter 5

Conclusions

This thesis makes contributions to the development of methods for polarimetric radar image processing. These methods are based on the matrix formalism.

The radar geometry can have its own influence in processing the polarimetric response, which led us to explore the monostatic and bistatic paradigms in Chapters 2 et 3. Full polarimetric diversity is generally assumed throughout the thesis. Nevertheless, a short example at the end of the Chapter 2 explores dual-polarisation results for a scene imaged at the same satellite pass by dual-pol monostatic and bistatic radar sensors. Differences in the interpretation of $H - \alpha$ parameters between dual and full polarimetry are studied and finally, monostatic and bistatic results in dual polarimetry are compared. In all other parts of the thesis, the full polarimetric model is used. The data is single look complex, with each pixel described by a scattering matrix, $\mathbf{S}$. This model is generally used for deterministic targets, while the vector formalism using the covariance matrix applies to computations involving distributed scatterers. The method proposed in Chapter 3 applies to a coherent target model, while the one proposed in Chapter 4 concerns the classification of real data, where inconsistent scatterers dominate.

5.1   Short summary and contributions

The main ideas presented in these chapters are resumed as follows:

- ■ **Chapter 3**:

  - • **Contribution 1:** *Method for detecting complex coneigenvalues, based on the real representation*

    The chapter begins with a detailed mathematical discussion of the conjugate similarity transformation: why it appears in PolSAR in relation to the BSA convention and what methods are known to perform this factorization. After introducing the Real Representation, we explain how

it can be used in the context of conjugate similarity for reciprocal and non-reciprocal scattering matrices. Reciprocal matrices have a unique factorization and experiments from this chapter show that the factors are the same as those obtained by a decomposition on the power matrix, $\mathbf{S}^H \mathbf{S}$. For non-reciprocal matrices, the factorization can provide solutions in the complex plane and at least one of the factors may not be unique.

- **Contribution 2:** *Analysis of real (monostatic) and simulated (monostatic and bistatic) polarimetric data using the real representation*

  In the second part, polarimetric simulations obtained using a full-wave electromagnetic computation software have been used. Such data has been generated for two coherent targets (a square metal plate and a right-angle dihedral) in monostatic and bistatic geometries, in each case considering a wide range of observation angles.

  The investigation using the eigen-decomposition of the real representation scattering matrix was applied to both simulated polarimetric data and real PolSAR datasets. It was shown that complex coneigenvalues may appear in both cases. The percentage is low (under 5%) for all tested monostatic data but becomes more significant with the bistatic observations.

- **Chapter 4**:

  - **Contribution 1:** *Analysis of the two factors in the polar decomposition*

    The first part of this chapter investigates the algebraic and geometric properties of the two polar factors. The Hermitian term can be assimilated as the rotation compensated, intensity preserving part of the scattering matrix.

  - **Contribution 2:** *Geometric clustering using the Hermitian factors*

    The embedding of Hermitian polar factors in the Riemannian manifold of positive-definite matrices is the main idea behind the proposed geometric clustering method. Proceeding the actual clustering, the Hermitian polar factors from fixed spatial neighborhoods have been "averaged" by a manifold-based gradient descent method, which estimates a geometric center of mass for the set of matrices in each neighborhood. This operation can be put in parallel to the estimation of sample covariance matrices by arithmetic averaging. The actual clustering has been implemented as a centroid, partitional-based algorithm having the AIRM Riemannian geodesic distance for intra/inter-cluster comparison. In light of this contribution, the method's performance has been tested using Hermitian factors from both real and simulated monostatic PolSAR

data. Compared to the nonsupervised Wishart method, improved quantitative and qualitative results are obtained. With real polarimetric data, the final clustering result is observed to better preserve texture details.

5.2 Perspectives for further developments

Extensions, as well as potential improvements, on each of the two main study axes of this thesis are discussed in this subsection.

- **Axis 1: Consimilarity and the Real Representation**

  - The investigation using simulated data did not identify a link between descriptors of the bistatic geometry (e.g., the bistatic angle) and the complex coneigenvalues. This may suggest that, if existent, the connection is multivariate, with improved models and tests needed.

  - An immediate extension of the work in Chapter 3 is to explore the (con)eigenvectors information (from the 2×2 scattering matrix, the 4×4 real representation matrix, or both). Descriptive parameters may be uncovered by the proposal of a new target vector model. In the current stage of development, the RR is restricted to coherent applications. Introducing a unique target vector model would allow its extension by a covariance-based incoherent decomposition technique.

    On a different note, machine learning models could be employed using features from the consimilarity factorization /the real representation.

- **Axis 2: The polar decomposition and geometric clustering**

  - The algebraic median is known to be a more robust estimate to outliers. Keeping the core ideas of the geometric clustering method, new tests may switch from the estimation of the Riemannian mean to the estimation of the Riemannian median [7].

  - Differently, the AIRM metric can be changed and compared with other distance metrics (e.g., the log-Euclidean), still adapted for the HPD manifold [29]. Also, the partitional-based clustering algorithm may be changed to other clustering models (e.g., hierarchical).

  - A much broader comparison between classical ICTD methods and the one proposed in the thesis would involve an understanding of the exact role carried by the manifold dimensions and the difference in informational content. This may take the form of comparing clustering results based on the scattering matrix (2×2) Hermitian factor, the PolSAR

(3×3) covariance and the (4×4) positive-definite factor from the polar decomposition of the real representation.

5.3 List of original publications

Journal articles:

- **[J1] M. Ciuca**, G. Vasile, A. Anghel, M. Gay and S. Ciochina, "*Bistatic Analysis Using the Real Representation Scattering Matrix Eigen-Classification*," in IEEE Transactions on Geoscience and Remote Sensing, vol. 60, pp. 1-18, 2022, Art no. 5228318, doi: 10.1109/TGRS.2022.3175475. **(Journal's Impact Factor IF 2022-2023: 8.125 - Q1)**

- **[J2] M. Ciuca**, G. Vasile, A. Anghel, M. Gay and S. Ciochina, "*Real Representation of the Polarimetric Scattering Matrix for Monostatic Radar*" in Remote Sensing, 2023, 15, 1037, https://doi.org/10.3390/rs15041037. **(Journal's Impact Factor IF 2022-2023: 5 - Q1)**

- **[J3]** A. Anghel, R. Cacoveanu, **M. Ciuca**, B. Rommen and S. Ciochina, "Multichannel Ground-based Bistatic SAR Receiver for Single-pass Opportunistic Tomography", in IEEE Transactions on Geoscience and Remote Sensing, 2023, doi: 10.1109/TGRS.2023.3294124. **(Journal's Impact Factor IF 2022-2023: 8.125 - Q1)**

- **[J4] M. Ciuca**, G. Vasile, M. Congedo and M. Gay, "*Riemannian Clustering of PolSAR Data using the Polar Decomposition*"
  under review (preprint: https://hal.science/hal-03839678v2)

Conference proceedings:

- **[C1] M. Ciuca**, A. Anghel, R. Cacoveanu, G. Vasile, M. Gay and S. Ciochina, "*Spaceborne Transmitter - Stationary Receiver Bistatic SAR Polarimetry - Experimental Results*", IEEE International Geoscience and Remote Sensing Symposium (IGARSS), 2020, pp. 3869-3872.

- **[C2] M. Ciuca**, A. Anghel, R. Cacoveanu, B. Rommen and S. Ciochina, "*Single-Pass Spaceborne Transmitter-Stationary Receiver Bistatic SAR Tomography - Novel Solution with 3 Imaging Channels*", IEEE International Geoscience and Remote Sensing Symposium IGARSS (IGARSS), 2020, pp. 124-127.

- **[C3] M. Ciuca**, G. Vasile, M. Gay, A. Anghel and S. Ciochina, "*Polarimetric Analysis Using the Algebraic Real Representation of the Scattering Matrix*", IEEE International Geoscience and Remote Sensing Symposium (IGARSS), 2021, pp. 499-502.

- **[C4] M. Ciuca**, G. Vasile, M. Gay, A. Anghel and S. Ciochina, "*Méthode générale de résolution de la similarité conjuguée en polarimétrie radar*" XXVI-IIème Colloque Francophone de Traitement du Signal et des Images, Sep 2022, Nancy, France.

- **[C5] M. Ciuca**, G. Vasile, M. Congedo, "Geometric Clustering of PolSAR Data using the Polar Decomposition", IEEE International Geoscience and Remote Sensing Symposium (IGARSS), 2023, pp. 1618-1621.

References

[1] (1983). IEEE Standard Definitions of Terms for Antennas. *IEEE Std 145-1983*, pages 1–31.

[2] (2014). IEEE Standard for Definitions of Terms for Antennas. *IEEE Std 145-2013 (Revision of IEEE Std 145-1993)*, pages 1–50.

[3] Ainsworth, T. L., Preiss, M., Stacy, N., Nord, M., and Lee, J.-S. (2007). Analysis of Compact Polarimetric SAR Imaging Modes. In *POLInSAR Workshop Proceedings*.

[4] Alonso-González, A., López-Martínez, C., Papathanassiou, K. P., and Hajnsek, I. (2020). Polarimetric SAR Time Series Change Analysis Over Agricultural Areas. *IEEE Transactions on Geoscience and Remote Sensing*, 58(10):7317–7330.

[5] Alonso-González, A., López-Martínez, C., and Salembier, P. (2014). PolSAR Time Series Processing With Binary Partition Trees. *IEEE Transactions on Geoscience and Remote Sensing*, 52(6):3553–3567.

[6] Barachant, A., Bonnet, S., Congedo, M., and Jutten, C. (2012). Multiclass Brain–Computer Interface Classification by Riemannian Geometry. *IEEE Transactions on Biomedical Engineering*, 59(4):920–928.

[7] Bhatia, R. (2013). *The Riemannian Mean of Positive Matrices*, pages 35–51. Springer Berlin Heidelberg, Berlin, Heidelberg.

[8] Cho, S. K. and Chu, C. M. (1989). Optimal Polarization in Bistatic Scattering. *SIAM Journal on Applied Mathematics*, 49(5):1473–1479.

[9] Ciuca, M., Vasile, G., Gay, M., Anghel, A., and Ciochina, S. (2022). Méthode Générale de Résolution de la Similarité Conjuguée en Polarimétrie Radar. In *GRETSI 2022 - XXVIIIème Colloque Francophone de Traitement du Signal et des Images*.

[10] Cloude, S. (1986). *Polarimetry - The Characterization of Polarization Effects in EM Scattering*. PhD thesis, Birmingham University.

[11] Cloude, S. (2009). *Polarisation: Applications in Remote Sensing*. Oxford University Press.

[12] Cloude, S. R. (2007). The Dual Polarization Entropy/Alpha Decomposition: A PALSAR Case Study.

[13] Deng, X., Lopez-Martinez, C., Chen, J., and Han, P. (2017). Statistical Modeling of Polarimetric SAR Data: A Survey and Challenges. *Remote Sensing*, 9(4).

References

[14] Formont, P., Ovarlez, J., Pascal, F., Vasile, G., and Ferro-Famil, L. (2011). On the Extension of the Product Model in POLSAR Processing for Unsupervised Classification using Information Geometry of Covariance Matrices. In *2011 IEEE International Geoscience and Remote Sensing Symposium*, pages 1361–1364.

[15] Formont, P., Ovarlez, J.-P., and Frédéric, P. (2013). *On the Use of Matrix Information Geometry for Polarimetric SAR Image Classification*. Springer Berlin Heidelberg, Berlin, Heidelberg.

[16] Germond, A.-L. (1999). *Theorie de la Polarimetrie Radar Bistatique*. PhD thesis, Nantes University.

[17] Graves, C. (1956). Radar Polarization Power Scattering Matrix. *Proceedings of the IRE*, 44(2):248–252.

[18] Haber, H. E. (2021). A Tale of Three Diagonalizations. *International Journal of Modern Physics A*, 36(04).

[19] Hong, Y. and Horn, R. A. (1989). A Characterization of Unitary Congruence. *Linear and Multilinear Algebra*, 25(2):105–119.

[20] Horn, R. A. and Johnson, C. R. (2013). *Matrix Analysis – Second Edition*. Cambridge University Press.

[21] Hubbert, J. C. (1994). A Comparison of Radar, Optic, and Specular Null Polarization Theories. *IEEE Transactions on Geoscience and Remote Sensing*, 32(3):658–671.

[22] Huynen, J. R. (1970). *Phenomenological Theory of Radar Targets*. PhD thesis.

[23] Ikramov, K. D. (2010). A Note on Complex Matrices that are Unitarily Congruent to Real Matrices. *Linear Algebra and its Applications*, 433(4):838–842.

[24] Jiang, T., Cheng, X., and Chen, L. (2006). An Algebraic Relation Between Consimilarity and Similarity of Complex Matrices and its Applications. *Journal of Physics: Mathematical and General*, 39:9215–9222.

[25] Jiang, T. and Wei, M. (2006). On the Reduction of a Complex Matrix to Triangular or Diagonal by Consimilarity. *Numerical Mathematics-English Series*, 15(2):107.

[26] Karnychev, V., Khlusov, V., Ligthart, L., and Sharygin, G. (2004). Algorithms for Estimating the Complete Group of Polarization Invariants of the Scattering Matrix (SM) Based on Measuring all SM Elements. *IEEE Trans. Geosci. Remote Sens.*, 42(3):529–539.

[27] Lankeit, J., Neff, P., and Nakatsukasa, Y. (2014). The Minimization of Matrix Logarithms: On a Fundamental Property of the Unitary Polar Factor. *Linear Algebra and its Applications*, 449:28–42.

[28] Lee, J.-S. and Pottier, E. (2009). *Polarimetric Radar Imaging: From Basics to Applications*. CRC Press - Taylor and Francisc Group.

[29] Lin, Z. (2019). Riemannian Geometry of Symmetric Positive Definite Matrices via Cholesky Decomposition. *SIAM Journal on Matrix Analysis and Applications*, 40(4):1353–1370.

[30] Ling, S. and Jiang, T. (2012). New Method for General Kennaugh's Pseudoeigenvalue Equation in Radar Polarimetry. *Front. Math. China*, 7(1):85–95.

[31] Lüneburg, E. and Boerner, W.-M. (1997). Homogeneous and Inhomogeneous Sinclair and Jones Matrices. In *Wideband Interferometric Sensing and Imaging Polarimetry*, volume 3120, pages 45–54. International Society for Optics and Photonics.

[32] Lüneburg, E., Cloude, S., and Boerner, W.-M. (1997). On the Pproper Polarimetric Scattering Matrix Formulation of the Forward Propagation versus Backscattering Radar Systems Description. In *Proc. IEEE Int. Geosci. Remote Sens. Symp. (IGARSS 1997)*, volume 4, pages 1591–1593 vol.4.

[33] Lüneburg, E., Morisaki, J., and Boerner, W.-M. (2004). On the Forward Scatter Alignment and the Backscatter Alignment Conventions of Bistatic Radar Polarimetry. In *Proceedings of ISAP*, volume 1, pages 1273–1276.

[34] Marino, A., Cloude, S. R., and Woodhouse, I. H. (2012). Detecting Depolarized Targets Using a New Geometrical Perturbation Filter. *IEEE Transactions on Geoscience and Remote Sensing*, 50(10):3787–3799.

[35] Neff, P., Nakatsukasa, Y., and Fischle, A. (2014). A Logarithmic Minimization Property of the Unitary Polar Factor in the Spectral and Frobenius Norms. *SIAM Journal on Matrix Analysis and Applications*, 35(3):1132–1154.

[36] Pang, B., Xing, S., Li, Y., and Wang, X. (2013). Novel Polarimetric SAR Speckle Filtering Algorithm Based on Mean Shift. *Journal of Systems Engineering and Electronics*, 24(2):222–223.

[37] Pang, B., Xing, S.-q., Li, Y.-z., and Wang, X.-s. (2012). Speckle Filtering Algorithm for Polarimetric SAR Based on Mean Shift. In *2012 IEEE International Geoscience and Remote Sensing Symposium*, pages 5892–5895.

[38] Pralon, L. (2016). *Scene Analysis and Interpretation by ICA Based Polarimetric Incoherent Target Decomposition for Polarimetric SAR Data*. PhD thesis.

[39] Souyris, J.-C. and Tison, C. (2007). Polarimetric Analysis of Bistatic SAR Images From Polar Decomposition: A Quaternion Approach. *IEEE Transactions on Geoscience and Remote Sensing*, 45(9):2701–2714.

[40] Touzi, R. (2007). Target Scattering Decomposition in Terms of Roll-Invariant Target Parameters. *IEEE Transactions on Geoscience and Remote Sensing*, 45(1):73–84.

[41] Trouvé, N. (2011). *Comparaison des Outils Optique et Radar en Polarimétrie Bistatique*. PhD thesis.

[42] Zhang, Y., Lai, X., Xie, Y., Qu, Y., and Li, C. (2021). Geometry-Aware Discriminative Dictionary Learning for PolSAR Image Classification. *Remote Sensing*, 13(6).

[43] Zhong, N., Yan, T., Yang, W., and Xia, G.-S. (2016). A Supervised Classification Approach for PolSAR Images Based on Covariance Matrix Sparse Coding. In *2016 IEEE 13th International Conference on Signal Processing (ICSP)*, pages 213–216.

[44] Zhong, N., Yang, W., Cherian, A., Yang, X., Xia, G.-S., and Liao, M. (2017). Unsupervised Classification of Polarimetric SAR Images via Riemannian Sparse Coding. *IEEE Transactions on Geoscience and Remote Sensing*, 55(9):5381–5390.